

# QSOs AND THE HARD X-RAY BACKGROUND

A. Vikhlinin

Space Research Institute, Russian Academy of Sciences  
Profsoyuznaya 84/32, Moscow 117810, Russia  
internet: vikhlinin@hea.iki.rssi.ru

August 16, 2002

**Abstract.** We calculate the contribution to the cosmic x-ray background (CXB) of a population of power law spectrum sources with spectral indices distributed over a broad range of values. The composite spectrum of this source population is significantly harder than that given by the power law having the average value of spectral indices. Starting from spectral distributions which are approximately those observed from quasars, it is possible to reproduce the CXB spectrum from  $\sim 0.5$  keV to  $\sim 20$  keV. If the spectra of quasars steepen at around 100 keV, the resulting composite spectrum nearly perfectly fits the CXB in the even broader energy range, up to  $\sim 100$  keV. The QSO population with broadly distributed spectral parameters is also characterized by a significant discrepancy between the results of hard and soft x-ray source counts. The same population of sources yields about three times more sources at 10 keV than at the corresponding flux at 1 keV, similarly to what is found from the comparison of HEAO A-1/Ginga and Einstein/ROSAT measurements. Thus, by allowing the spectra of QSO's to span a broad range of spectral indices, it is possible to reproduce both the CXB spectrum and account for the apparent differences in number counts in different energy bands.

**Key words:** X-rays: general – Cosmology: diffuse radiation – quasars: general

---

## 1. Introduction

In spite of great progress in the study of the cosmic x-ray background (CXB) radiation achieved since its discovery more than 30 years ago (Giacconi et al. 1962) its origin remains unclear. In the soft x-ray band, deep ROSAT source counts show that the population of faint x-ray sources (of them some 70% are QSOs, Boyle et al. 1993) is able to account for the main portion (if not 100%) of the soft x-ray (1-2 keV) background, while the contribution of a truly diffuse component (such as the hot intergalactic gas) must be less than 25% at 90% confidence (Hasinger et al. 1993).

At harder x-rays, 3-60 keV, sensitive imaging surveys have not yet been performed, and the main efforts have been concentrated on explaining the CXB spectrum which is remarkably well fit by the thermal bremsstrahlung model with  $kT = 40$  keV (Marshall et al. 1980). The COBE limit on the Comptonization parameter excludes the possibility of a uniform hot medium producing more than a few percent of the CXB in the harder x-ray band (Mather et al. 1990). Hence, most likely the hard x-ray background is also composed by unresolved compact sources (see the discussion of the “spectral coincidence” and the contribution of point sources to the CXB in Giacconi & Zamorani 1987).

The main difficulty with the discrete source explanation of the hard x-ray background has been that there is no known source population whose spectra resemble that of the CXB. Clusters of galaxies, which are as numerous as AGNs at high fluxes in the standard x-ray band (Piccinotti et al. 1982), typically have thermal bremsstrahlung spectra with temperatures of about 6 keV (David et al. 1993), and exhibit negative cosmological

---

*Send offprint requests to:* A. Vikhlinin

evolution (e.g., Gioia et al. 1990). Hence, they cannot be significant contributors to the broad-band x-ray background. Population of AGN's which dominate the soft x-ray source counts and exhibit positive cosmological evolution have 2–20 keV spectra significantly steeper than the x-ray background. HEAO A-1/EXOSAT/Ginga observations of low luminosity AGNs (mostly Seyfert 1 galaxies) revealed a “canonical”  $\alpha = 0.7$  spectrum (Mushotzky 1984), to be compared with the energy index of 0.4 for the CXB in this energy band. Both soft and hard x-ray observations of high luminosity AGNs (mostly quasars) suggested that there was no universal power law for this class of sources. Observed spectral indices are distributed from  $\alpha \sim 0$  to  $\alpha \sim 2.0$ , with the mean value of about 1 in the soft x-rays and 0.8–0.9 in the 2–10 keV x-ray band (Williams et al. 1992, Comastri et al. 1992, and Wilkes & Elvis 1987). The average spectral index of quasars also corresponds to a spectrum which is significantly softer than that of the CXB, which was used to argue that their contribution to the hard x-ray background could not exceed  $\sim 10\%$  (Fabian, Canizares, & Barcons 1989).

In this paper we show that it is still possible to make a significant portion of the hard x-ray background from QSOs, i.e. that the observed composite spectrum of quasars can be as hard as the CXB spectrum. The basic idea relies on the observed broad spread of QSO spectral indices. X-rays observed from QSOs at energy  $E$  are emitted at higher energies,  $(1+z)E$ . Therefore, distant objects with flat spectra appear brighter than those with steep spectra, and hence, it follows that the mean spectrum hardens with increasing redshift even though no true spectral evolution occurs. A similar effect arises if soft x-ray luminosities do not correlate with spectral properties. The absence of such a correlation implies that hard spectrum sources should be on average more luminous in the 2–10 keV x-ray band than the steep spectrum sources. Furthermore, the broad distribution of spectral indices provides a natural explanation for the mismatch between the results of soft and hard x-ray source counts found from the comparison of Einstein/ROSAT and HEAO A-1/Ginga surveys. Since hard sources are brighter at high redshifts than soft ones, a difference in number-flux relations determined at, for example, 1 keV and 10 keV is expected, with larger surface number density at the hard energy band.

In section 2 we argue that it is necessary to account for the contribution of QSOs in source models of the x-ray background. Models of the QSO population (spectra, luminosity function, and the cosmological evolution) used in the paper are described in section 3. Basic equations used for calculations of the composite QSO spectrum and the number-flux relations in different energy bands are derived in section 4. Section 5 presents the results of calculations. The main results of the paper are briefly discussed in section 6.

## 2. QSOs, Seyfert 1s, and the CXB

The difficulties with the explanation of the CXB spectrum by AGNs arise from the assumption that their spectra are simple power laws over a broad energy range. Schwartz & Tucker (1988) have shown that if AGN spectra flatten with increasing energy up to some energy cutoff, these difficulties can be overcome and it is possible to match the CXB spectrum by the composite spectrum of unresolved distant AGNs. In fact, the spectral flattening was observed in Ginga spectra of Seyfert 1 galaxies and was interpreted as either the partial covering by cold material of a power law x-ray spectrum or as reprocessed emission from cold material (Piro et al. 1989, Matsuoka et al. 1990, Pounds et al. 1990). GRANAT and OSSE observations of a sample of Seyfert 1s revealed that their spectra do steepen again at energies of about 50–100 keV (Jourdain et al. 1992, Johnson et al. 1994). Thus the observed spectra of Seyfert 1s are quite close to what is required by the model of Schwartz & Tucker (1988) – the source spectra flatten above  $\sim 10$  keV and they steepen again at about 100 keV. This stimulated Zdziarski et al. (1993) to claim that it is AGNs with Seyfert 1-like spectra which comprise the 2–100 keV x-ray background. In fact, using the cosmological evolution model of Boyle et al. (1993) and the model spectrum determined from Ginga/OSSE observations of Seyfert 1s Zdziarski et al. (1993) obtained an excellent fit to the CXB spectrum in the 2–100 keV energy range.

However, the explanation of the CXB by Seyfert 1 galaxies may fail because, as discussed by Giacconi & Zamorani (1987), the contribution of known classes of steep spectrum sources must also be included in modeling the CXB spectrum such as quasars and clusters of galaxies. Giacconi & Zamorani showed that if the contribution of the  $\alpha \sim 0.7 - 1$  sources to the soft x-ray background amounts to at least 50% of the CXB, the residual CXB spectrum is much flatter than the  $kT = 40$  keV spectrum. Therefore, it may be difficult to fit the residual CXB spectrum by spectra of Seyfert 1 galaxies.

Deep, soft surveys show that the contribution of QSO's to the CXB is in fact significant. ROSAT deep surveys show that point-like faint sources contribute the bulk of the 2 keV CXB, with the directly resolved fraction being about 60%. From fluctuation analyses, point sources contribute about 75% of the CXB and a reasonable extrapolation of the number-flux relation to even fainter fluxes can account for 100% of the soft x-ray background (Hasinger et al. 1993). In a deep ROSAT survey, Boyle et al. (1993) identify 64% of the extragalactic

x-ray sources with QSOs and this number can be as high as  $\sim 80\%$ . Hence, it seems very likely that QSOs contribute not less 50% of the 2 keV CXB, and consequently their contribution cannot be overlooked in any model of the CXB.

QSO spectra are generally less well studied than those of Seyfert 1 galaxies. Both soft and hard x-ray observations show that spectral indices of quasars are distributed over a broad range of values, from  $\alpha \sim 0$  to  $\alpha \sim 2$ , and the mean spectral index in the 2-10 keV band is 0.8-0.9 (Comastri et al. 1992, Williams et al. 1992). In their review of x-ray observations of AGNs, Mushotzky, Done & Pounds (1993) discuss the difference between 2-10 keV spectra of Seyfert 1 galaxies and quasars. *Ginga* spectra show that the radio-loud QSOs do not require additional reflection components and, apart from 3C273 and PHL 1657, show no deviations from a simple power law over the 2–20 keV energy band (Williams et al. 1992). The radio-quiet QSO spectra do show deviations from the power law but the steeper underlying spectrum ( $\alpha \approx 1.0$ ) implies a real difference between radio-quiet QSOs and Seyfert 1 galaxies. We conclude that QSOs are different from Seyfert Is from the point of view of x-ray spectra and show less evidence for spectral flattening above 10 keV. Therefore, it is necessary to subtract the contribution of QSOs to the x-ray background before fitting the CXB spectrum by spectra of Seyfert Is. If we assume that QSOs all have the  $\alpha = 0.8 - 0.9$  spectrum and contribute about 50% to the 2 keV background, the spectrum of the residual background will be much harder than the  $kT = 40$  keV spectrum (Giacconi & Zamorani 1987), which will be difficult to fit even with spectra of Seyfert Is with significant reflection contributions.

### 3. Models of The Source Population

We consider four models of the source population to reconstruct the CXB spectrum and to illustrate properties of the reconstruction – “realistic” (model **A**), “reduced realistic” (**B**), “pure” (**C**), and “common” (**D**). Model spectra are single power laws modified at the soft and the hard energies to describe a soft excess and a high energy cutoff:

$$F(E) = \begin{cases} a_s E^{-\alpha_s} & E < E_s \\ a_m E^{-\alpha_m} & E_s < E < E_h \\ a_h E^{-\alpha_h} & E > E_h \end{cases} \quad (1)$$

In the standard x-ray band (2-10 keV) we assume that sources have power law spectra, with no additional features such as strong emission lines, absorption edges, or a reflection component, and have spectral indices distributed according to a Gaussian distribution with the mean value of 0.8 and the dispersion of 0.35. “Unphysical” energy spectra with negative spectral indices are prohibited in the model by a cutoff of the distribution at zero. The choice of parameters is based on the results of *EXOSAT* and *Ginga* measurements of spectra of subsamples of soft x-ray selected high luminosity AGN (Comastri et al. 1992, Williams et al. 1992). Both sets exhibit a steep 2-10 keV mean spectral index (0.81 for *Ginga* and 0.89 for *EXOSAT* data), with a wide range of spectral indices, distributed from 0.08 to 1.26, with an intrinsic dispersion of about 0.3. There is evidence of a soft excess in QSO energy spectra below an energy of a few keV (Wilkes & Elvis 1987, Comastri et al. 1992, Fiore et al. 1994), manifesting itself as a gradual steepening of source spectra in softer energy bands. Hence, we introduce the soft excess to the model spectra as an additional power law below 1 keV, with the mean soft x-ray spectral index of 1.4. The choice of a mean soft x-ray spectral index is motivated by ROSAT measurements of bright QSO spectra in the energy band of 0.1-2.4 keV (Laor et al. 1994).

The bulk of sources in the model have spectral indices less than 1, which yields infinite broad band luminosities. Therefore, the break in spectra at high energies is required. We introduce such a break at around 100 keV by steepening the spectral index up to the value of 2.0. The cutoff energy of 100 keV is chosen so that it is possible to reproduce the CXB spectrum up to  $\sim 100$  keV, rather than this choice is motivated by the observations of QSO spectra.

Parameters of the soft excess and the high energy cutoff are distributed according to a Gaussian distribution with a dispersion equal to 0.3 of the mean value. For the high energy cutoff, the extremely low values of the break energy (below 30 keV) and flat spectra (with the hard spectral index less than the main spectral index) are prohibited.

The four models differ by the distribution of spectral parameters. In the “realistic” model **A** all the spectral parameters are characterized by Gaussians. The “reduced realistic” model **B** is used to show how the range in the soft excess and the high energy cutoff parameters influence the composite spectrum; the soft excess parameters are held fixed at a value of 1.4 for the spectral index and 1 keV for the break energy, and the high

energy cutoff parameters at values of 2.0 for the spectral index and 100 keV for the break energy. The “pure” model **C** is used to demonstrate the effects of the soft excess and the high energy cutoff and is characterized by single power law spectra over the whole energy range with a distribution of spectral indices analagous to that in the model **A**. Finally, in the “common” model **D** all parameters are held fixed which corresponds to the assumption of an identical spectrum for all sources.

We assume further that there is no correlation between the spectral properties and the luminosity in the soft x-ray band. This would of course imply the existence of a negative correlation between the luminosity in the harder x-ray band (2-10 keV) and the spectral index, i.e. hard sources must be on average more luminous in this band. Existing x-ray data do not enable one to explore the existence of such a correlation with high confidence, since the 2-10 keV x-ray spectra are measured only for the several dozens of the brightest quasars. However, Williams et al. (1992), found a negative correlation between the x-ray luminosity and 2-10 keV spectral index at more than 90% significance in their sample of 13 high-luminosity AGNs, while Wilkes & Elvis (1987) find no correlation between the x-ray luminosities and spectral indices measured in the 0.3-3.5 keV band. Finally, recent ROSAT measurements indicate that quasar intensities are much less scattered at around 0.3 keV than at higher energies (Laor et al. 1994).

For the model luminosity function we use the QSO soft x-ray luminosity function derived by Boyle et al. (1993) from the joint analysis of the deep ROSAT survey, and the EMSS luminosity function. At  $z = 0$ , this luminosity function can be represented as two power laws, with a break at  $L_X^* = 10^{43.9}$  erg s<sup>-1</sup> in the 0.3-3.5 keV energy band,  $\Phi(L_X) \propto L_X^{-3.4}$  above the break, and  $\Phi(L_X) \propto L_X^{-1.7}$  below the break. Boyle et al. (1993) also derive the cosmological evolution of QSOs which can be described as pure luminosity evolution,  $L_X \propto (1+z)^K$ , with  $K = 2.8$  for  $\Omega = 0$  and  $K = 2.5$  for  $\Omega = 1$  universe (Boyle et al. 1993). For  $\Omega = 1$  a “cut off” in the evolution is required at around  $z = 2$ . We use the same model of cosmological evolution for the values of  $\Omega$  ranging from  $\Omega = 0$  and  $\Omega = 1$  in our calculations, with  $K = 2.7$ , and cutoff of evolution at  $z = 3.0$ .

It must be emphasized that no spectral evolution is present in calculations. This means that, by assumption, the distribution of spectral parameters is the same at every redshift.

#### 4. Basic Equations

If at the source rest-frame the source spectrum is given as  $A S_0(E)$ , and the source lies at a redshift  $z$ , then the observed energy flux density (flux per unit energy interval) is:

$$f(E) = \frac{A S_0(E(1+z))}{4\pi(a_0 r)^2(1+z)}, \quad (2)$$

where  $r(z, \Omega)$  is the angular size distance,

$$a_0 r(z, \Omega) (H_0/c) = \frac{2}{\Omega^2(1+z)} \{ \Omega z + (\Omega - 2) [\sqrt{1 + \Omega z} - 1] \} \quad (3)$$

(Mattig 1958). For power law spectra,  $S_0(E) = E^{-\alpha}$ , eq. 2 becomes:

$$f(E) = \frac{A E^{-\alpha} (1+z)^{-\alpha-1}}{4\pi(a_0 r)^2}. \quad (4)$$

If sources are distributed homogenously in space and there is no density evolution, the number of sources per unit redshift increment is

$$\frac{dN}{dz} = n_0 \frac{4\pi c^3}{H_0^3} z^2 \frac{4[\Omega z + (\Omega - 2)(\sqrt{1 + \Omega z} - 1)]^2}{\Omega^4 z^2 (1+z)^3 \sqrt{1 + \Omega z}} = n_0 \frac{4\pi c^3}{H_0^3} z^2 \xi(z, \Omega) \quad (5)$$

where  $n_0$  is the volume number density at  $z=0$  (Mattig 1958).

Einstein and ROSAT observations indicate that the observed properties of the high luminosity AGN population require a cosmological evolution which can be described in terms of pure luminosity evolution, i.e. the luminosity scales with redshift as  $L_x(z) = L_x(0) C(z)$ , with  $C(z) = (1+z)^K$  (Boyle et al. 1993). For this type of evolution the  $z$ -dependence of the luminosity function is:

$$\Phi(L_x, z) = \frac{1}{C(z)} \Phi\left(\frac{L_x}{C(z)}, 0\right) \quad (6)$$

Available x-ray data on the luminosity function and its evolution is derived from observations in the 0.3-3.5 keV energy band. For simplicity, we assume that the the same relations apply to 1 keV luminosities;  $L_1$  is denoted as the 1 keV luminosity in the source rest-frame.

Using equations 2-6 we calculate the composite energy spectrum of the source population, and the results of source counts as a function of energy band. The spectral parameter  $\alpha$  is used to designate different spectral shapes. For a class of power-law spectra  $\alpha$  is simply the power-law index; for more complicated spectral shapes  $\alpha$  becomes a vector of parameters, and integrals over the range of  $\alpha$  indicate integrals over different spectral shapes. The assumed absence of any correlation of spectral properties with redshift or with soft x-ray luminosity (section 3) means that the density distribution of the spectral parameter,  $\alpha$ , is a function of  $\alpha$  only, i.e. the probability that  $\alpha$  is within the interval  $(\alpha, \alpha + d\alpha)$  is

$$dP = W(\alpha) d\alpha \quad (7)$$

Different spectral shapes are denoted as  $S_0(E, \alpha)$ , with this function normalized to unity at 1 keV, so that the energy flux density at a particular energy  $E_0$  is given by  $L_1 S_0(E_0, \alpha)$ , where  $L_1$  is the 1 keV source luminosity.

#### 4.1. Composite Spectrum

In this section we calculate the composite spectrum of sources uniformly distributed in space, with spectral properties described above, and pure luminosity evolution. Let us first find the mean energy spectrum of sources located at a redshift  $z$ . This can be evaluated by integration of equation 2 over the appropriate range of luminosities and spectral shapes:

$$F_z(E) = \int_0^\infty \Phi(L_1, z) dL_1 L_1 \int_\alpha W(\alpha) d\alpha \frac{S_0(E(1+z), \alpha)}{4\pi (a_0 r)^2 (1+z)} \quad (8)$$

For pure luminosity evolution the luminosity function changes with redshift following eq.6, and the evaluation of the integral over  $L_1$  in eq.8 yields:

$$F_z(E) = \bar{L}_1 \frac{C(z)}{4\pi (a_0 r)^2 (1+z)} \int_\alpha W(\alpha) d\alpha S_0(E(1+z), \alpha) \quad (9)$$

where  $\bar{L}_1$  is the mean present day soft x-ray luminosity and  $C(z)$  is the cosmological luminosity evolution function.

It is easy to show that equation 9 implies that the composite spectrum of sources at a given  $z$  hardens with increasing redshift. Let the source spectra be described as a simple power law, i.e.  $S_0(E, \alpha) = E^{-\alpha}$ . Then equation 9 becomes

$$F_z(E) \propto \int_\alpha W(\alpha) d\alpha E^{-\alpha} (1+z)^{-\alpha} \quad (10)$$

The spectral index of the composite spectrum (as a function of energy) is the logarithmic derivative of the spectral flux:

$$\begin{aligned} \bar{\alpha} &= -\frac{d \log F_z(E)}{d \log E} = -\frac{E}{F_z(E)} \frac{d F_z(E)}{d E} \\ &= \frac{\int_\alpha \alpha W(\alpha) E^{-\alpha} (1+z)^{-\alpha} d\alpha}{\int_\alpha W(\alpha) E^{-\alpha} (1+z)^{-\alpha} d\alpha}, \end{aligned} \quad (11)$$

i.e. the initial distribution of spectral indices,  $W(\alpha)$ , must be replaced by  $W(\alpha) E^{-\alpha} (1+z)^{-\alpha}$  when one observes sources at a redshift  $z$  and an energy  $E$ . Thus, the distribution is weighted towards flatter spectra at higher energies and redshifts.

On multiplying eq.9 by  $dN$ , the number of sources in the redshift interval  $(z, z + dz)$  (eq. 5), and integrating over redshift, we find the expression for the composite spectrum of the source population:

$$F(E) = \left(\frac{c}{H_0}\right)^3 n_0 \bar{L}_1 \int_0^\infty dz \frac{\xi(z, \Omega) z^2}{(a_0 r)^2 (1+z)} C(z) \int_\alpha W(\alpha) d\alpha S_0(E(1+z), \alpha). \quad (12)$$

This equation is used in section 5.1 for calculations of the composite spectrum of QSOs, using models **A-D** for the spectral parameter distributions.

#### 4.2. Source counts at different energies

The 1 keV luminosity of a source whose energy flux density observed at the energy  $E_0$  is  $f$  can be calculated (cf. eq2) as:

$$L_1 = \frac{4\pi (ar_0)^2 (1+z)}{S_0(E_0(1+z), \alpha)} f \quad (13)$$

The fraction of sources of a given spectrum, at a given redshift yielding an observed flux greater than  $f$  is calculated by integrating the luminosity function:

$$n' = \int_l^\infty \Phi(L, z) dL \quad (14)$$

where the lower limit,  $l$  is the limiting luminosity for a given flux,  $f$ :

$$l = \frac{4\pi (a_0r)^2 (1+z)}{S_0(E_0(1+z), \alpha)} f. \quad (15)$$

For pure luminosity evolution the redshift dependence of the luminosity function is given by eq.6, and the above equation becomes:

$$n' = \int_{l/C(z)}^\infty \Phi(L, 0) dL \quad (16)$$

The number-flux relation is obtained by multiplying equation 16 by the number of sources in the redshift interval (eq. 5) and integrating over redshift:

$$N(> f) = n_0 \frac{4\pi c^3}{H_0^3} \int_0^\infty dz \xi(z, \Omega) z^2 C(z) \int_\alpha W(\alpha) d\alpha \int_{l/C(z)}^\infty \Phi(L, 0) dL \quad (17)$$

To compare results of source counts at different energies it is necessary to express these fluxes in terms of a common energy band. It is common practice to do this using the mean source spectrum (known or assumed). Let us denote  $S(E, \alpha_0)$  as the mean source spectrum (i.e. corresponding to some mean value of the spectral parameters). The corresponding transformation of the observed energy flux density  $f(E)$  at energy  $E$  to flux,  $F$ , in the energy band  $(E_1, E_2)$  is:

$$F = f(E) \frac{\int_{E_1}^{E_2} S(E, \alpha_0) dE}{S(E, \alpha_0)} \quad (18)$$

Equations 17 and 18 can be used to calculate difference between the soft and hard x-ray source counts, for example, at 1 and 10 keV.

## 5. Results

In this section we present results of calculations of the CXB spectrum and the number-flux relation in different energy bands for four models of spectra distribution (Section 3) and several values of the density parameter,  $\Omega$ . No qualitative difference is found in results of calculations performed for different values of the cosmological density parameter,  $\Omega$ , ranging from 0 to 1. When presenting the results we will simply point out the trend of changing the derived relationships for  $\Omega$  increasing from 0 to 1 and will not emphasize the dependence of the results on the density parameter.

Composite spectra of the source populations derived for models **A** through **D** are shown in Fig.1. These spectra are obtained by integrating (eq.12) over redshifts from 0 to 10. The assumption that sources are still bright at very high redshifts is of course uncertain. However, we use the model for cosmological evolution in which the growth of luminosity ceases at a redshift of 3 (section 3), and redshift effects rapidly make the contribution of sources at higher redshifts negligible (cf. eq.9).

Models with a broad distribution of spectral parameters and the high energy cutoff (**A** and **B**) perfectly reproduce the CXB spectrum from  $\sim 1$  to  $\sim 60 - 100$  keV. Model **C**, without the high energy cutoff, predicts further flattening of the CXB spectrum above  $\sim 20$  keV, but yields the correct slope of the spectrum in the 2-10 keV energy band. The “standard” model **D**, without any scattering of spectral parameters, reproduces the well-known result – the average QSO/AGN spectrum is too steep to fit the CXB spectrum in the energy range from 2-10 keV. Below  $\sim 2$  keV all models predict a steepening of the CXB spectrum, which is not related to the presence of a soft excess in individual spectra. For example, model spectrum **C**, without any soft excess lies very close to spectra **A** and **B** (with soft excess below 1 keV) above 0.7-1 keV.

In the harder x-ray band, above  $\sim 20$  keV, a high energy cutoff is required in source spectra to fit the CXB spectrum. For an  $\Omega = 0$  Universe, in the context of the present model, the break must be at around 100 keV; this value gradually decreases to 70 keV for  $\Omega = 1$  (see trend of model spectra with increasing  $\Omega$  indicated by the arrow in Fig. 1). The broad distribution of the high energy spectral index (model **A**) reproduces the flattening of the CXB at  $\geq 300$  keV. However, there is a lack of spectral data on QSO’s at such high energies. Not only are the particular values of the cutoff energies unknown, but the very existence of breaks in QSO spectra is not very well established (Mushotzky, Done, & Pounds 1993). For this reason, we avoid adjusting the spectral shapes at high energies to reproduce the detailed shape of the CXB spectrum.

## 5.2. *Source counts*

We calculated the source number-flux relations at three different energies, 1, 5, and 10 keV, by Monte-Carlo integration of eq.17. Source fluxes at these energies were transformed to 2-10 keV fluxes by means of eq.18, using the average source spectrum (i.e. the spectrum defined by mean values of parameters in the appropriate model). The results are presented in Fig. 2. Models **A** and **B**, which are distinguished by Gaussian distribution of the soft excess parameters, yield essentially the same results, and therefore, only model **B** is presented in Fig. 2.

Models with broad distributions of spectral parameters predict a significant difference between the results of hard and soft x-ray source counts. In the EMSS flux range,  $10^{-13} - 10^{-12}$  ergs  $s^{-1} cm^{-2}$ , there are approximately three times more sources observed from the same population at 10 keV than at the corresponding 1 keV flux. We emphasize that this effect does not arise from the presence of any spectral features (like a soft excess). Model **C**, having a simple power law spectrum for individual sources, predicts almost the same difference in hard and soft x-ray source counts, as does model **B**, with the soft excess. As can be expected, model **D** predicts number-flux relations to be the same at all energies. The agreement is partially distorted if the soft spectral component which we assumed to be present below 1 keV starts at higher energies. In this case, the soft excess in spectra of faint sources is shifted to low energies. As a result, when using the  $z = 0$  average spectrum for flux transformations, the 2-10 keV flux is underestimated, which causes an artificial decrease in the soft x-ray source counts relative to hard x-ray counts. Calculations show however, that in the EMSS flux range,  $10^{-13} - 10^{-12}$  ergs  $s^{-1} cm^{-2}$ , the difference is less than a factor of 1.3 if a soft excess starts at energies of about 3 keV.

## 6. Discussion

In this paper we have shown the importance of the distribution of spectral parameters in calculations of the contribution of any source population to the x-ray background. Of known classes of potential contributors to the CXB, quasars demonstrate probably the broadest distribution of spectral parameters, with 2-10 keV power law indices ranging from  $\sim 0$  to  $\sim 1.5 - 2$ . Using models of QSO spectra distributed closely to what is observed, we have shown that the composite spectrum of faint QSOs can be significantly harder than that given by the average value,  $\sim 0.8$ , of the spectral index. In fact, the composite spectrum of the QSO population closely mimics the 0.5-100 keV CXB spectrum, if one assumes the existence of a high energy cutoff in QSO spectra at around 100 keV. Another important effect which is readily reproduced, when source spectra span a broad

range, is the difference between the results of hard and soft x-ray source counts. The same population of sources yields about three times more sources at around 10 keV than at the corresponding 1 keV flux.

The key point of our spectral distribution models is that the soft x-ray luminosity, at around 1 keV, does not correlate with other spectral properties of sources. This means that hard sources are brighter at higher energies than soft sources, and this actually accounts for approximately half the effect of hardening required to reproduce the CXB spectrum; redshift effects serve to enhance the effect. As was discussed in Section 3, available x-ray observations can neither prove nor disprove this assumption, and this is obviously the weak point of the described model. Although the existence of a characteristic energy at which quasar luminosities and spectra are not correlated does not seem unreasonable, its particular value of 1 keV was chosen partially for the sake of simplicity and partially because of the wish to reproduce the CXB spectrum as well as possible. At the time of this writing it was generally accepted that the CXB intensity in the soft x-ray band is in excess over the  $E^{-0.4}$  extrapolation from higher energies. Note that models **A** through **C** spectra show  $\sim 40 - 50\%$  excess over the  $E^{-0.4}$  spectrum in the 1 – 2 keV energy band, which is in agreement with ROSAT measurements of the CXB spectrum (Hasinger 1992). Later ASCA measurements (Gendreau et al. 1994), on the contrary, show that CXB follows the  $E^{-0.4}$  spectrum down to at least 1 keV. Our model still can fit this spectrum (without the “soft excess”), provided that quasar luminosities are uncorrelated with spectra at lower energies, 0.1 – 0.3 keV, as is suggested by Laor et al. (1994).

This paper assumes that the high energy break in QSO spectra occurs at around 100 keV. With this value of the break energy it is possible to reproduce the CXB spectrum in the very broad energy range from 0.5 to about 100 keV, if the cosmological density parameter,  $\Omega$  is zero. To reproduce the CXB spectrum in  $\Omega = 1$  Universe a break energy of about 70 keV is required, in good agreement with the break energy of 50-100 keV observed by OSSE in low luminosity AGNs, mostly Seyfert 1s (Johnson et al. 1994).

Summarizing, the paper shows that quasars still may be considered as the main contributors to the broad-band x-ray background. It also shows the importance of relaxing the assumption that all source have the same spectrum when the source population is characterized by significant distribution of spectral shapes.

*Acknowledgements.* The author would like to thank R.Sunyaev for his friendly criticism. Special thanks to W.Forman for his great help in work on the manuscript.

## References

- Boyle B.J., Griffiths, R.E., Shanks, T., Steward G.C., and Georgantopoulos, I. 1993, MNRAS, 260, 49.  
Comastri, A., Setti, G., Zamorani, G., Elvis, M., Giommi, P., Wilkes, J., & McDowell, J., 1992, ApJ, 384, 62.  
David, L.P., Slyz, A., Jones, C., Forman, W., Vrtilik, S.D., Arnaud, K.A., 1993, ApJ, 412, 479  
Fabian, A.C., Canizares, C.R., & Barcons, X. 1989, MNRAS, 239, 15.  
Fiore, F., Elvis, M., Siemiginowska, A., Wilkes, B.J. & McDowell, J.C. 1994 ApJ in press.  
Gendreau, K., et al. 1994, “New Horizons of X-ray Astronomy – First Results from ASCA”, preprint.  
Giacconi, R., Gursky, H., Paolini, F., and Rossi, B. 1962, Phys. Rev. Letters, 9, 439.  
Giacconi, R., & Zamorani, G. 1987, ApJ, 313, 20.  
Gioia, I.M., Henry, J.P., Maccacaro, T., Morris, S.L., & Stocke, J.T. 1990, ApJ, 356, L35.  
Hasinger, G. 1992, in: The X-ray Background, X. Barcons & A.C. Fabian eds. (Cambridge University Press), p.1.  
Hasinger, G., Burg, R., Giacconi, R., Hartner, G., Schmidt, M., Trümper, J., & Zamorani, G., 1993, A&A, 275, 1.  
Johnson, W.N. et al., 1994, in the AIP Conference Proceedings 304, eds. C. Fitchel, N. Gehrels, J. Norris, 515.  
Jourdain, E., et al. 1992, A&A, 256, L38.  
Laor, A., Fiore, F., Elvis, M., Wilkes, B., & McDowell, J.C., 1994, ApJ, 435, 611.  
Marshall, F. et al. 1980. ApJ, 235, 4.  
Mather, J. et al. 1990, ApJ, 354, L37.  
Matsuoka, M., Piro, L., Yamauchi, M., and Murakami, T. 1990, ApJ, 361, 440.  
Mattig, W. 1958, Astron.Nachr. 284, 109.  
Mushotzky, R.F., 1984, Adv. Space. Res., 3, 10.  
Mushotzky, R.F., Done, C., & Pounds, K. 1993, Ann. Rev. Astr. & Ap., 31, 717.  
Nandra, K., & Pounds, K.A., 1994, MNRAS, 1994, 268, 405.



- Piccionotti, G., Mushotzky, R.F., Boldt, E.A., Holt, S.S., Marshall, F.E., Serlemitsos, P.J., and Shafer, R.A. 1982, ApJ, 253, 485.
- Piro, L., Matsuoka, M., and Yamauchi, M. 1989, Proc. 23rd ESLAB Symposium on "Two Topics in X-ray Astronomy", ESA SP-296, 819.
- Pounds, K., Nandra, K., Stewart, G., George, I., and Fabian A. 1990, Nature, 344, 132.
- Schwartz, D. and Tucker, W. 1988, ApJ, 332, 157.
- Wilkes, B. and Elvis, M. 1987, ApJ, 323, 243.
- Williams, O.R. et al., 1992, ApJ, 389, 157.



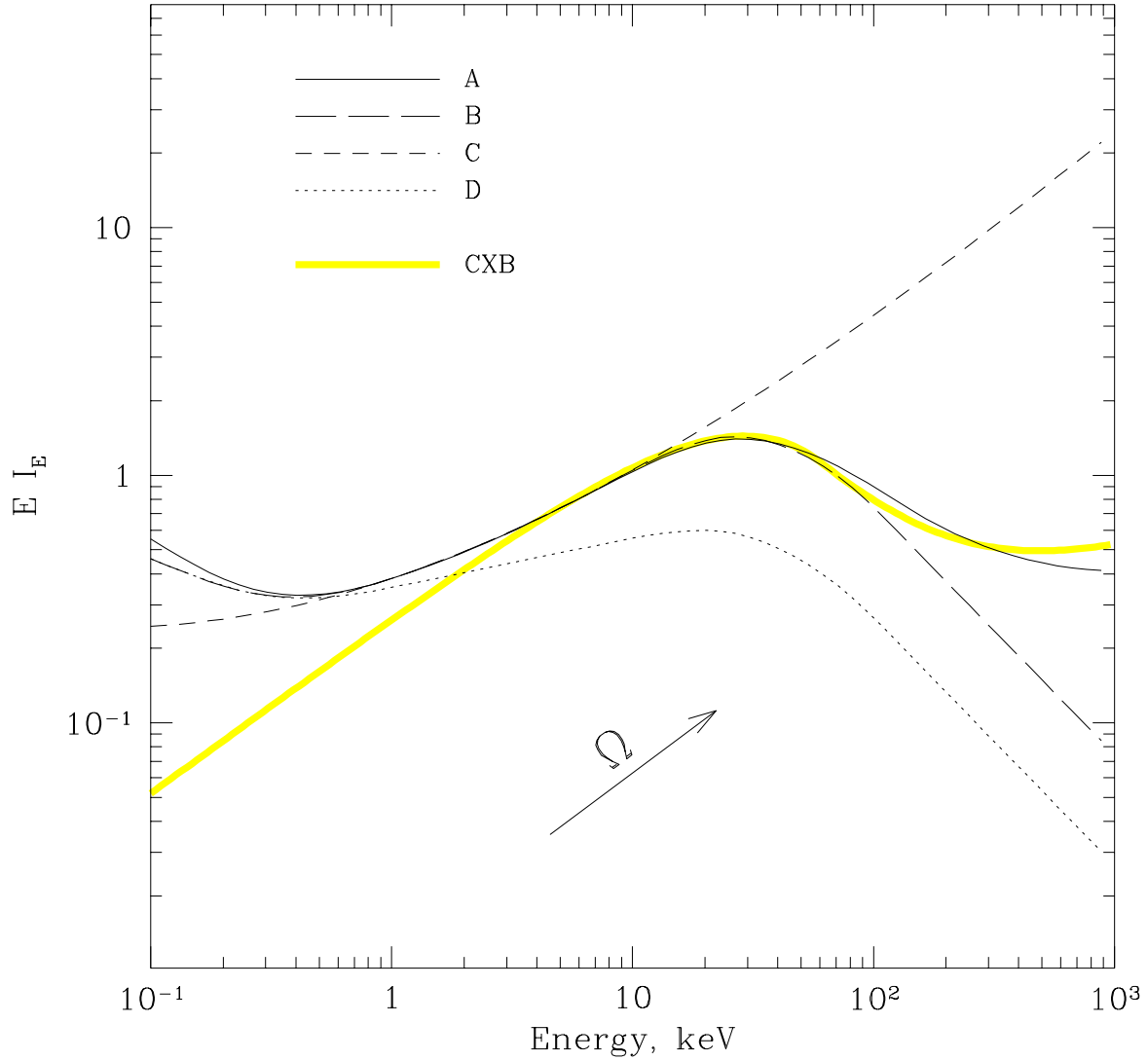


**Fig. 1.** The composite spectrum calculated for models **A-D**, and the x-ray background spectrum. The absolute normalization of model spectra is arbitrary. All models with the scattering of spectral parameters (**A-C**) adequately describe the CXB spectrum from  $\sim 2$  to more than 10 keV. Models with the high energy cutoff at around 100 keV (**A** and **B**) succeed in describing the CXB spectrum up to 60-100 keV. Model **D**, without any scattering of the spectral parameters, reproduces the well known result: the mean spectrum of QSOs is too steep to fit the CXB spectrum in the 2-10 keV energy band. The model spectra deviate from the hard x-ray background extrapolation at energies below 2-2.5 keV. Note that the models with and without the soft excess in source spectra (**A** & **B**, and **C**, respectively) yield almost the same spectra above  $\sim 1$  keV. The arrow shows the trend of model spectra when the density parameter,  $\Omega$ , increases.

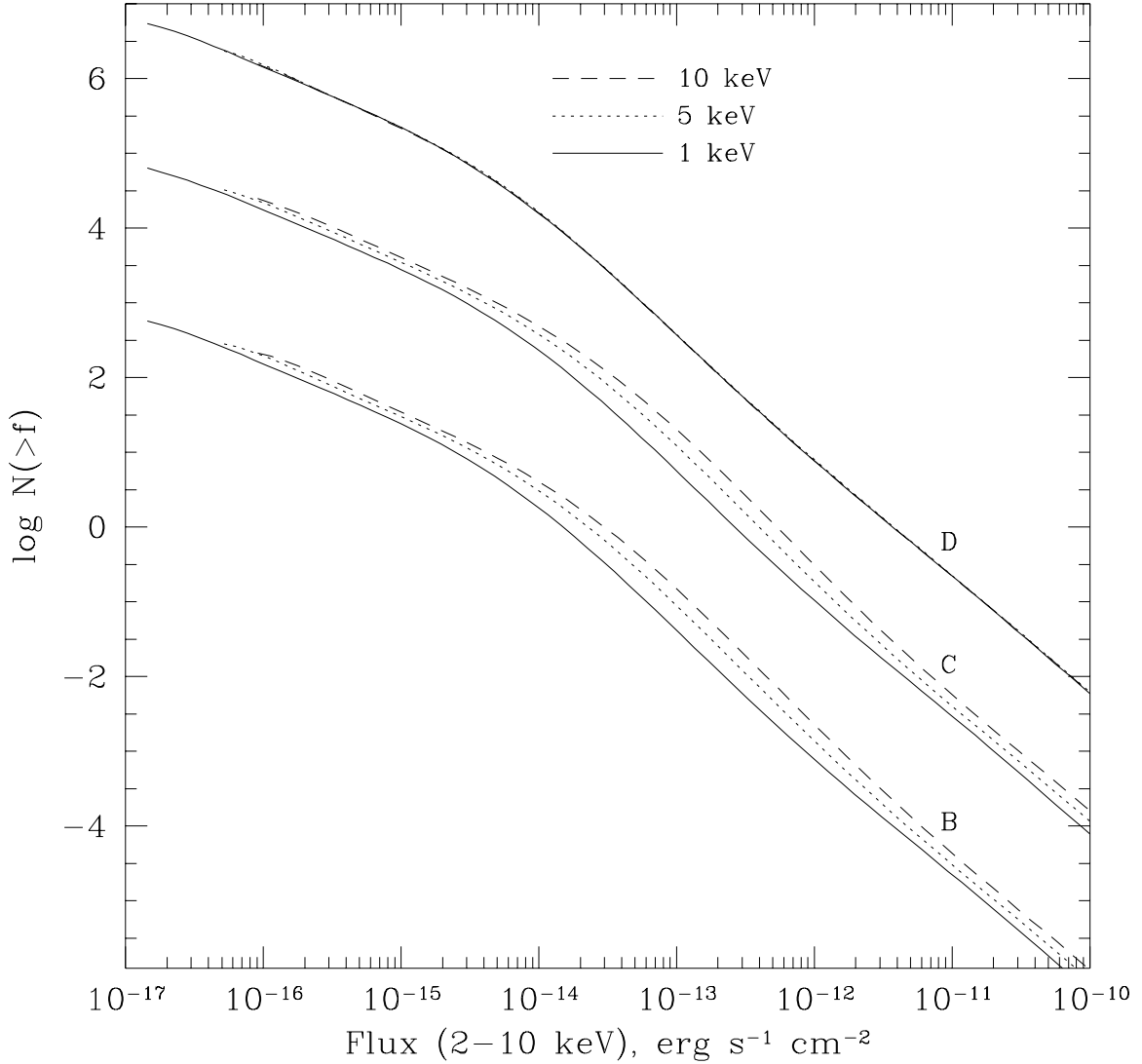


**Fig. 2.** Source number-flux relation at three energies, 1, 5, and 10 keV, calculated for different models of source spectra distribution. Normalizations are arbitrary. For models with scatter of spectral parameters (**B** and **C**) hard x-ray source counts yield more than two times more sources than the observations performed at 1 keV; in the EMSS flux range,  $10^{-13} - 10^{-12} \text{ ergs s}^{-1} \text{ cm}^{-2}$ , the difference is approximately a factor of three for both models with and without the soft excess (**B** and **C**, respectively). Model **D**, with the soft excess and without any scattering of spectral parameters, predicts perfect agreement between soft and hard x-ray source counts.